Accepted for publication in the Astrophysical Journal
Preprint typeset using LaTeX style emulateapj

A DEEP SEARCH WITH *HST* FOR LATE TIME SUPERNOVA SIGNATURES IN THE HOSTS OF XRF 011030 AND XRF 020427

Andrew Levan[1,2,3], Sandeep Patel[1,4], Chryssa Kouveliotou[1,5] Andrew Fruchter[1,3], James Rhoads[3], Evert Rol[1,2], Enrico Ramirez-Ruiz[1,6,7], Javier Gorosabel[3,8], Jens Hjorth[9], Ralph Wijers[10], W. Michael Wood-Vasey[11], David Bersier[3], Alberto Castro-Tirado[8], Johan Fynbo[9], Brian Jensen[9], Elena Pian[12], Nial Tanvir[1,13], Stephen Thorsett[14], Stan Woosley[1,14]

Accepted for publication in the Astrophysical Journal

ABSTRACT

X-ray Flashes (XRFs) are, like Gamma-Ray Bursts (GRBs), thought to signal the collapse of massive stars in distant galaxies. Many models posit that the isotropic equivalent energies of XRFs are lower than those for GRBs, such that they are visible from a reduced range of distances when compared with GRBs. Here we present the results of two epoch *Hubble Space Telescope* imaging of two XRFs. These images taken approximately 45 and 200 days post burst reveal no evidence for an associated supernova in either case. Supernovae such as SN 1998bw would have been visible out to $z \sim 1.5$ in each case, while fainter supernovae such as SN 2002ap would have been visible to $z \sim 1$. If the XRFs lie at such large distances, their energies would not fit the observed correlation between the GRB peak energy and isotropic energy release ($E_p \propto E_{iso}^{1/2}$), in which soft bursts are less energetic. We conclude that, should these XRFs reside at low redshifts ($z < 0.6$), either their line of sight is heavily extinguished, or they are associated with extremely faint supernovae, or, unlike GRBs, these XRFs do not have temporally coincident supernovae.

Subject headings: gamma rays: bursts

1. INTRODUCTION

X-ray Flashes (XRFs) occupy the extreme left (lower energy) wing of the peak energy distribution of Gamma-Ray Bursts (GRBs). While GRBs radiate the majority of their energy in γ-rays ($E_p \sim 200$ keV, Preece *et al.* 2000), XRFs are characterized by peak energies below 50 keV and an X-ray fluence in excess of that observed in γ-rays. XRFs were discovered with the *BeppoSAX* Wide Field Cameras (Heise *et al.* 2001a); they constitute approximately 1/3 of the total burst population (Lamb *et al.* 2004). The physical mechanisms driving XRFs and their observed differences to GRBs are some of the key questions in the field today.

Of the many competing theories relating to the origin of XRFs, the most popular is that XRFs are produced when a classical GRB is observed "off-axis", so that the highly collimated ejecta (i.e., the highest energies and harder photons) are not seen (Yamazaki, Ioka & Nakamura, 2002; Rhoads 2003; Dado et al. 2004). Alternatively, models invoking either an increase of the baryon load within the fireball itself (Dermer, Chiang & Böttcher 1999; Ramirez-Ruiz & Lloyd-Ronning 2002; Meszaros *et al.* 2002; Huang, Dai & Lu 2002) or low efficiency (high baryon load) shocks (Zhang & Meszaros 2002; Barraud et al. 2003) can also produce XRFs.

One interesting consequence of all of the models above, is that they predict a distance distribution for XRFs which is foreshortened with respect to that of GRBs, since XRFs emit a fraction of the energy of the GRB itself. This hypothesis seems to be supported by the analysis of GRBs with known redshifts, whereby the event peak energy (E_p)

[1]Institute for Nuclear Theory, University of Washington, Seattle, Washington 98195-1550, USA
[2]Department of Physics and Astronomy, University of Leicester, University Road, Leicester, LE1 7RH, UK
[3]Space Telescope Science Institute, 3700 San Martin Drive, Baltimore, MD21218, USA
[4]Universities Space Research Association, National Space Science Technology Center, SD-50, 320 Sparkman Drive, Huntsville, AL 35805, USA
[5]NASA/Marshall Space Flight Center, National Space Science Technology Center, SD-50, 320 Sparkman Drive, Huntsville, AL 35805, USA
[6]School of Natural Sciences, Institute for Advanced Study, Einstein Drive, Princeton, NJ 08540, USA
[7]Chandra Fellow
[8]Instituto de Astrofísica de Andalucía (IAA-CSIC), P.O. Box 03004, E-18080 Granada, Spain.
[9]Astronomical Observatory, University of Copenhagen, Juliane Maries Vej 30, DK-2100, Copenhagen, Denmark
[10]Astronomical Institute "Anton Pannekoek"and Center for High Energy Astrophysics, University of Amsterdam, Kruislaan 403, 1098 SJ Amsterdam, NL
[11]Lawrence Berkeley National Laboratory, One Cyclotron Road, Mailstop 50R232, Berkeley, CA 94720, USA
[12]INAF, Osservatorio Astronomico di Trieste, Via G.B. Tiepolo 11, I-34131 Trieste, I
[13]Centre for Astrophysics Research, University of Hertfordshire, College Lane, Hatfield AL10 9AB, UK
[14]Department of Astronomy & Astrophysics, University of California at Santa Cruz, Santa Cruz, CA 95064, USA

scales as $E_{iso}^{1/2}$, i.e. softer GRBs have lower isotropic energies (Amati *et al.* 2002; Lloyd-Ronning & Ramirez-Ruiz 2002). Qualitative arguments on XRF distances were presented by Kouveliotou *et al.* (2004), where a comparison of the energetics of the X-ray afterglows of GRBs and XRFs suggested that were the latter placed a high redshift (e.g. $z = 1.5$), their luminosities would rival those of the brightest GRBs, suggesting a closer proximity for XRFs.

Qualitative distance arguments have also been presented by Kouveliotou *et al.* (2004), where a comparison between the energetics of GRBs and XRFs indicated that if XRFs were placed further than $z = 1.5$ their luminosities would exceed those of the brightest GRBs, suggesting a closer proximity for XRFs.

However, determining the true distances of XRFs has proven to be exceptionally difficult observationally. Only two XRFs have so far been associated with optical afterglows, XRF 020903 (Soderberg *et al.* 2004) and XRF 030723 (Fynbo *et al.* 2004). Of these only the former has a measured spectroscopic redshift ($z = 0.25$; Soderberg *et al.* 2004) while the latter has only a redshift limit ($z < 2.3$) with the suggestion of low redshift based on the presence of a supernova like component it its late time light curve (Fynbo *et al.* 2004). A second possible case, GRB/XRF 031203 is not yet settled, as there is an ongoing debate on the true nature of this nearby event ($z = 0.105$), which was originally classified as an XRF (Watson *et al.* 2004) based on its X-ray brightness as inferred from the discovery of a halo from dust scattering in our own Galaxy (Vaughan *et al.* 2004). However, an analysis of its high energy spectrum recorded with *INTEGRAL* (Sazonov *et al.* 2004) revealed an $E_p \sim 190$ keV, apparently inconsistent with that inferred from the dust halo. The paucity of distance measurements thus prevents us from deriving definitive conclusions on the XRF distance distribution.

The spectroscopic signatures of type Ic supernovae seen in GRB 030329/SN 2003dh (Stanek *et al.* 2003; Hjorth *et al.* 2003), and the discovery of photometric bumps in many GRB optical afterglow light curves (e.g. Zeh, Klose & Hartmann 2004), strongly support the collapsar model (Woosley 1993), whereby the majority of long duration GRBs are the result of core collapse supernovae. Should XRFs be associated with supernovae, as seen in GRBs, but found at typically lower redshifts, it should be possible to constrain their distances by the detection of a supernova brightening in their X-ray located host galaxies. This can be the case where an optical afterglow is seen (e.g. XRF 030723; Fynbo *et al.* 2004) or in some cases where there was no apparent optical afterglow (e.g., this was recently the case for GRB/XRF 031203 (Bersier *et al.* 2004; Thomsen *et al.* 2004;Cobb *et al.* 2004; Gal-Yam *et al.* 2004; Malesani *et al.* 2004)).

Here we present results on our *HST* data of two XRF host galaxies, identified earlier by a combination of *HST* and *Chandra* data (Fruchter *et al.* 2002a,b; Bloom *et al.* 2003). In the present study, we concentrate on the difference imaging between two *HST* epochs separated by six months, and the constraints these results place on underlying supernovae. Finally we combine these results with the properties of the X-ray lightcurves of each XRF and their similarities with GRBs to reach conclusions on the likely nature of XRFs.

2. OBSERVATIONS

XRF 011030 was detected with *BeppoSAX* on 2001 October 30, 06:28:02 UT (Gandolfi 2001) within an initial error circle of $r = 5'$. It had a long duration ($t_{90} \sim 1000s$; for a definition of t_{90} see Kouveliotou *et al.* 1993), an apparently low E_p (< 40 keV; Heise *et al.* 2001b) and a fluence of 9×10^{-7} ergs cm^{-2} ($2 - 28$ keV). We imaged the region surrounding XRF 011030 with the WIYN 3.5m telescope on 2001 November 1, 2, and 3, reaching limiting magnitudes of R$\sim$ 23.5 on each occasion. Image subtraction failed to locate any afterglow candidates to these limits; a stacked image indicated that no optical afterglow was present to R>24 (Rhoads *et al.* 2001). Likewise, other optical observations taken by several groups also failed to identify any afterglow candidates. Radio observations with the VLA, however, did identify a fading source as the possible afterglow of XRF 011030 (Taylor *et al.* 2001). The field was imaged by *Chandra* at two epochs on 2001 November 9 (47.21 ks) and 29 (20.12 ks), with the Advanced CCD Imaging Spectrometer S-array (ACIS-S). Comparison of the two epochs revealed a variable source within the *BeppoSAX* error box at at RA =20:45:36.00, DEC =+77:06:01.09 (Harrison *et al.* 2001; Bloom *et al.* 2003), approximately $1\farcs2$ from the location of the radio source; the *Chandra* source was then identified as the X-ray counterpart of XRF 011030 (Fruchter *et al.* 2002a).

XRF 020427 was detected also with *BeppoSAX* on 2002 April 27, 3:48:40 UT and was classified as an XRF by its $10 - 28$ to $2 - 10$ keV hardness ratio, which indicated an X-ray rich event (in't Zand *et al.* 2002). Optical observations taken after the burst failed to locate the afterglow to a limit of I=21.7, 51 hours after the burst (Jakobsson *et al.* 2004) .We observed the field of XRF 020427 on 2002 May 11 with the 1.54m Danish Telescope at La Silla, Chile in the R-band with a total exposure time of 9× 300 seconds (Table 1) and place a limit of I>22.0 for any optical afterglow at this time. Radio observations of the XRF field also failed to find any counterpart (Wieringa *et al.* 2002). XRF 020427 was imaged with the *Chandra* ACIS-S array on 2002 May 6 (13.92 ks) and 14 (14.76 ks). Comparison of the two observations revealed a bright, rapidly declining source within the *BeppoSAX* error circle at RA = 22:09:28.22, Dec=-65:19:32.03 (Fox 2002a,b; Bloom *et al.* 2003). VLT observations of the counterpart obtained in June 2002 show a blue colour complex of galaxies underlying the position of the X-ray transient (Castro-Tirado *et al.* 2002). Amati *et al.* (2004) presented a comprehensive analysis of all available X-ray data on this burst. The prompt event had an $E_p < 5$ keV and a duration $t_{90} \sim 60$s, and its fluence was 5.8×10^{-7} ergs cm^{-2} ($2 - 28$ keV); the best fitting pseudo-redshift was $0.1 < z < 0.2$ (Atteia 2003; see also section 4).

For each XRF we reprocessed the *Chandra* data, extracted the XRF spectra and generated a response using *CIAO* version 3.0.2 and *CALDB* version 2.26. We searched both images in a region $4.2' \times 4.2'$ (512 × 512 pixels) centered at the *BeppoSAX* source location; within this radius, there is only one clearly decaying source, already identified as the XRF afterglow. We used a source extraction region

of 2″ radius centered on each XRF location to extract spectra in both epochs, and we fit the spectra simultaneously with an absorbed power law model. For each burst we used the C-statistic (appropriate for low count data; Cash *et al.* 1979); the spectra were unbinned and the (negligible) background was not subtracted. The resulting counts, spectral indices and fluxes are shown in Table 1.

In the following we use our WIYN and Danish 1.5m images of XRF 011130 and 020427, respectively, to facilitate the alignment of the *Chandra* observations to the *HST* field.

3. *HST* OBSERVATIONS

XRF 011030 was observed with *HST* on 2001 December 12 and again on 2002 June 12. The first of STIS observations were obtained in both the 50CCD and Long-Pass (LP) filters, while the second was obtained only with 50CCD. The field of XRF 020427 was imaged with *HST* also using STIS in the 50CCD mode 2002 June 10 and 14; LP images were also obtained at the June 14 epoch. A final epoch was obtained on 2002 October 26, again using the 50CCD filter. Table 2 shows the log of the *HST* observations. Both XRF datasets were retrieved from the *HST* archive[15] and were combined and cosmic ray cleaned using the drizzle routine (Fruchter & Hook 2002). Dithered images were drizzled onto a grid with pixels of size 0.″025, half the native STIS pixel, using a value for `pixfrac` of 0.7. All observations were aligned with the IRAF routine `geomap` using point sources in common in each *HST* image and then redrizzled onto an aligned output grid. A log of *HST* and all ground based optical observations is shown in Table 2.

3.1. *Astrometric Alignment*

To accurately position the *Chandra* sources on the *HST* image the *Chandra* field has to be precisely aligned with that of *HST*. The STIS FOV of only 50″ typically contains an insufficient number of sources to assure such an alignment and, therefore, it is necessary to use ground based intermediate images. Here we used data obtained at the WIYN (XRF 011030) and Danish 1.5m (XRF 020427) telescopes. Each of these fields was initially aligned to the USNO-A2 catalog and positions were estimated for all objects for which an apparent optical counterpart was identified within 0.″5 of a *Chandra* source. A first alignment of the X-ray to the optical sky was then performed using the *Chandra* header coordinates. Finally, we performed relative astrometry between our ground based observations and the HST images, using eight and ten common point sources between each field (for XRF 011030 and 020427, respectively). As a result, we could place the X-ray counterparts of XRF 011030 and 020427 onto our *HST* images with a positional accuracy of $\sim 0.''2$ and $0.''15$, respectively.

Our positions agree with those reported by Fruchter *et al.* (2002a,b) and Bloom *et al.* (2003) and confirm their identification of the host galaxies. The positions of the X-ray afterglows for both XRFs are coincident with the stellar fields of their host galaxies with blue global colors (Bloom *et al.* 2003). The host of XRF 020427 also appears to have several neighbour galaxies of similar magnitude, color and morphology indicating that it may be part of a galaxy group. The blue colors of each XRF host galaxy are similar to those of other GRB hosts, and imply relatively young stellar populations and little dust (see e.g. Trentham *et al.* 2002; Le Floc'h *et al.* 2003; Christensen *et al.* 2004).

To search for optical variability of the X-ray sources, we performed direct image subtractions between the *HST* epochs for each XRF (two for XRF 011030 and three for XRF 020427). To increase the depth of our final subtraction for XRF 020427 we also drizzled the data of June 10 and 14 together onto a single first epoch image. We then searched the resulting difference image using SExtractor (Bertin & Arnouts 1998) with a signal to noise threshold of 5σ and a Gaussian mask with FWHM = 3 pixels, to mimic the *STIS* point spread function (PSF); no variable object was found in either field, with the exception of saturated stellar objects, which leave clearly detectable residuals. Our subtractions are shown in Figure 1. To define the depth of our subtractions, we created artificial stars within the first epoch image with magnitudes in the range $27 < V < 30$, and a FWHM equal to the PSF in our *STIS* images. We then performed the subtraction of the final from the initial epoch and searched the resulting difference image for variable sources using the same method described above. We recovered 100% of the artificial stars at $V = 28.7$ in the XRF 020427 image, and 95% of those at $V = 28.5$ in the XRF 011030 field (at a 5σ detection level).

This sensitivity difference is mostly due to a larger number of saturated objects in the field of XRF 011030 than for XRF 020427; when our artificial stars land on (or near) these objects, we are unable to recover them. Moreover, the depth of XRF 011030 images is slightly lower. The "true" limit for XRF 011030 further diminishes to $V \sim 27.6$ when the large foreground extinction (E(B-V) = 0.4) towards this source is considered. For XRF 020427 the smaller extinction (E(B-V)=0.03) has little effect on the limiting magnitude. We discuss the limits these observations place on the optical afterglow and underlying supernova emission in the next section.

3.2. *Lack of residual optical emission at 40 days after the burst trigger*

Assuming that there is a supernova associated with each XRF, the flux seen at the location of any burst at a given time is the sum of the afterglow, supernova and host galaxy. The host galaxy component can be removed by the subtraction of a late time image after both afterglow and SN have faded. For GRBs with bright optical afterglows their magnitude at $\delta t = 10$ days after trigger, is in the range $22 < R < 25$ (see e.g. Fig 2. Fox et al. 2003); assuming a fast decaying trend (t^{-2}) this would imply that the majority of these afterglows would be somewhat brighter than $R = 28$ after 40 days. In the case of XRF 011030 and 020427 the putative sum of afterglow + SN at 40 days is fainter than $V \sim 28.5$. This is not overly surprising however, since many GRB afterglows are often

[15] http://archive.stsci.edu

not seen at optical wavelengths (so called "dark" bursts), and therefore a more careful examination is necessary to determine if this lack of emission is unusual.

Under the standard fireball model (see Mészáros 2002 for a review) GRB afterglows are described by a synchrotron spectrum, which can be represented to first order by a set of gradual power-laws with breaks at frequencies representing the cooling of the fireball (ν_c), the peak frequency of the electrons (ν_p) and the self-absorption frequency where the fireball becomes optically thick (ν_{sa}). It is therefore possible to extrapolate between wavebands under the premises of this model. Such extrapolations are potentially of great value since they predict the expected optical flux in a GRB and may differentiate between truly dark events and the ones which are not seen due to insufficient depth of the observations (Fynbo *et al.* 2001). Groot *et al.* (1998) first attempted such a method for the dark GRB 970828 and found that extrapolating the X-ray slope into the optical regime predicted significant optical flux, while none was seen. However, such predictions need to take account of the possible presence of ν_c between the optical and X-ray frequencies and therefore a range of possible slopes becomes necessary; thus the distinction between dark and bright bursts is not sharp but is populated with "gray" bursts, events which fall between the extremes of the extrapolations (Rol *et al.* 2004). Applying the same method of extrapolation to XRF 011030 and 020427, we find that the existing optical limits for both bursts lie below the most optimistic estimates from the X-ray afterglow of each burst, but above the limits derived using a worst case scenario (the most rapid possible decay and the presence of a cooling break between optical and X-ray bands). Thus these non-detections can be explained without recourse to additional extinction (and always assuming a fireball spherical expansion); this is evident in Figure 2, where we show that the observed optical limiting flux for XRF 020427 falls well within the extrapolation of the limits obtained from the X-rays. For more details of this method, the reader is referred to Rol *et al.* (2004).

We now proceed to examine the frequency of SN detection in GRB afterglows. Since the discovery of the first such event (GRB 980425/SN 1998bw; Galama *et al.* 1998) many low redshift ($z < 1$) afterglows have been found with indications of supernovae signatures in their light curves (e.g. Zeh, Klose & Hartmann 2004). These supernova are thought to be the results of core collapse of massive stars (e.g., Wolf-Rayet stars) that have lost much of their hydrogen (and possibly helium) envelopes prior to collapse and therefore form Type Ib/c supernovae (Woosley 1993; MacFadyen & Woosley 2000). The recent spectroscopic discovery of supernovae associated GRBs in 2003 (GRB 030329; Hjorth *et al.* 2003; Stanek *et al.* 2003, GRB 031203; Malesani *et al.* 2004) strongly supports this model. An observational consequence of a GRB-SN association is that, since supernovae reach their maximum light a few weeks after the core collapse (which is thought to trigger the GRB), their emergence in the lightcurve can slow or even reverse the fading of the optical afterglow. More importantly, in some cases they may also be visible even where an optical afterglow is not (e.g. SN 1998bw/GRB 980425; SN2003lw/GRB/XRF 031203; Galama *et al.* 1998; Bersier *et al.* 2004; Cobb *et al.* 2004; Gal-Yam *et al.* 2004; Malesani *et al.* 2004; Thomsen *et al.* 2004).

To determine the limits on underlying supernovae for each XRF, we therefore created spectral templates based on the SN 1998bw spectra first reported by Patat *et al.* (2001)[16]. Since our observations at a fixed observer time correspond to different rest frame times, for each redshift considered we chose the template spectra taken closest to the rest frame time corresponding to the observer time of the *HST* data. In cases where temporally coincident spectra were not available, we used the closest available spectra normalized against the observed photometry of SN 1998bw at that time (using the light curves of Galama *et al.* 1998) and K-corrected them to the appropriate redshift corresponding to the fixed observer time. We then determined the measured counts from these spectra within the STIS/50CCD passband by convolving them with the STIS response with *synphot*. At this stage we also folded in the effect of Galactic extinction for each XRF field based on the E(B-V) from Schlegel, Finkbeiner & Davis (1998). This allows us to obtain the expected number of counts from a SN 1998bw like supernova for each XRF field at various redshifts.

The optical spectra available for SN 1998bw extend only to $\sim$ 3000Å. Therefore they are of limited use at higher redshifts, where we observe the rest frame ultraviolet component. Moreover, very few studies exist to date of the UV-spectra of type Ic supernovae, in particular temporally resolved studies, which would be ideal for our comparisons (a generic feature of most supernovae is a supression of the UV-flux due to the blanketing effect of metals). We have attempted therefore, to estimate limits on the UV flux via two methods. The first is to assume zero flux below 3000Å (rest frame); while this is clearly underestimating the true flux, it provides a firm lower limit on the expected brightness of the supernova within our redshift limits. The second method is to use the available UV spectroscopy of SN 2002ap (a typical Ic supernova), taken with *STIS* on 2002 February 1 using the G230L grism. This spectroscopy shows a substantial decrease in flux from $\sim 3000 - 2000$ Å as expected and also seen in SN 1994I (Millard *et al.* 1999). We have rescaled the flux here for our purposes so that it matched the flux seen with ground based spectra at $\sim$ 3000Å. Although these spectra should provide a reasonable measure for the UV flux for type Ic supernovae, we also note that the spectrum of SN 2002ap was taken at an early epoch ($\sim$ 5 days) and possible evolution of the features may change the spectral shape at later epochs. However, as time resolved UV spectroscopy is not available for any high velocity Type Ic, we cannot determine if this early shape is maintained into later epochs.

SN 1998bw was a very bright Type Ic event; fainter Type Ic supernovae are more common locally and it is likely that their overall distribution may be bimodal (Richardson *et al.* 2002). Although it is not clear that all Type Ic supernovae produce a GRB, the ones firmly (i.e. spectroscopically) associated with GRBs are comparable in brightness

[16]These templates were taken from the suspect SN database http://tor.nhn.ou.edu/~ suspect/index.html

to SN 1998bw (e.g. Hjorth *et al.* 2003; Stanek *et al.* 2003; Garnavich *et al.* 2003). The lack, however, of a supernova in GRB 010921 to a limit of 1.34 magnitudes fainter than SN 1998bw (Price *et al.* 2003) and the best fit of both GRB 020410 and XRF 030723 with a supernova ~ 2 magnitudes fainter than SN 1998bw (Levan *et al.* 2004a; Fynbo *et al.* 2004) imply that we may be seeing a broader luminosity function for the GRB associated supernovae. Low redshift ($z < 1$) GRBs show a moderate (~ 1 magnitude) dispersion in the peak luminosity of their supernovae (Thomsen *et al.* 2004; Zeh, Klose, & Hartmann 2004). The faintest of the local high-velocity type Ic supernovae is SN 2002ap. This supernova exhibits similar spectral and temporal evolution to SN 1998bw (with a slightly faster rising lightcurve, e.g. Fig 4 of Foley *et al.*. 2003) and was 2 magnitudes fainter than SN 1998bw although still one magnitude brighter than the faintest type Ic ever seen (Richardson *et al.* 2002). We have, therefore chosen to use this supernova as a template to study what might be expected as a limiting magnitude from fainter supernovae. Our predicted magnitudes are not strongly dependent on the UV-flux below $z \sim 1$ as can be seen in Figures 3 & 4 (upper panels), where we plot the evolution of the magnitude of SN 1998bw and SN 2002ap at various redshifts in the two XRF fields, respectively. However the limiting magnitude beyond this is a sensitive function of the unknown UV-flux, and the true magnitude may be somewhat different; a hard upper limit is set by our assumption of zero UV flux.

The evolution of the expected magnitudes for supernovae with differing properties are shown in Figures 3 & 4 (for XRF 011030 and 020427 respectively). For XRF 011030 a faint type Ic supernova association, such as SN 2002ap, would fall below the detection limit of our observations at $z \sim 1$, while a SN 1998bw type would have been seen out to $z \sim 1.5$. For XRF 020427 both supernovae would be visible up to $z \sim 1.2$, and again only a SN 1998bw type could be seen beyond $z \sim 1.5$. However, for $z > 1$ the rest frame UV light from the supernova is very sensitive to the host galaxy extinction, such that a moderate $A_V \sim 1$ could extinguish the supernova contribution (see also Figures 3,4, lower panels). Further, the true colors of type Ic supernovae are not well constrained in the rest frame UV. For most supernovae the colors evolve from blue to red, with bluer bands experiencing peak light before the red. Some supernovae associated with GRBs, however, have exhibited blue (rest-frame UV) peak colors (e.g., SN2001ke/GRB 011121; Garnavich *et al.* 2003; Greiner *et al.* 2003) implying that they have a significant UV-component, while many Type Ic supernovae (including SN 1994I and SN 2002ap) have a large UV decrement due to metal line blanketing. Our approach, therefore places only a lower limit on the expected emission from supernovae at these redshifts.

The limiting magnitudes placed on underlying supernova depend not only on the observed spectra but also on the shape of the light curve of the associated supernova. Local type Ib/c supernova show a range of light curve properties including some which evolve faster than SN 1998bw (e.g. SN 1994I) and some which evolve slower (e.g. SN 1997ef). A fast evolving supernova would have decayed further at the time of our observations, while a slower one would be closer to peak (or even at peak if viewed at higher redshifts). To explore the possible effect of light curve shape on our limits we performed the same K-corrections as described above but on supernovae which evolved 30 % slower, and 30 % faster than SN 1998bw. In each case we maintained the UV-flux estimates for SN 2002ap. A faster evolving supernova would drop below our visibility limit at $z \sim 0.8$ for XRF 011030 and at $z \sim 1.1$ for XRF 020427, assuming the same peak magnitude with SN 2002ap at $M_V = -17.2$. A slower evolving supernova (again with a peak brightness similar to the one of SN 2002ap) would be seen out to $z = 1.3$ and $z = 1.5$ for XRF 011030 and 020427, respectively. It should also be noticed that our estimates assume that the supernova light at the time of our second epoch observations is much fainter than at the first. This is so far the case for *all* type Ib/c SNe known (for example SN 1998bw would have fallen by more than a factor 10 in the period between the observations considered here); it is clear, however, that our estimates depend on the SNe light curve shape and would provide different limits in the (unlikely) event of e.g., SNe light curves exhibiting a plateau.

4. DISCUSSION

The X-ray light curve decay indices (assuming a power law decay starting at $t = 0$ for each burst) are $\alpha = -2.0 \pm 0.3$ and $\alpha = -1.4 \pm 0.4$ for XRF 011030, 020427, respectively. These slopes are both comparable to those observed in typical GRB X-Ray afterglows, which at late times lie in the range $-1 < \alpha < -2$ with a best fit of $\alpha = -1.69$ (Kouveliotou *et al.* 2004). Unfortunately our sample of known redshift XRF afterglows with multi-epoch X-ray imaging is very limited with a possible exception of the still debated GRB/XRF 031203, which exhibits a large X-ray flux as well as a high peak energy (Vaughan *et al.* 2004; Watson *et al.* 2004; Sazonov *et al.* 2004). The fluxes observed for XRF 011030 and 020427 are also similar to the typical GRB fluxes at $z \sim 1$ at similar epochs. For either XRF afterglow, however, to have a luminosity similar to GRB 980425 or GRB/XRF 031203 they would have to be exceptionally close ($z \sim 0.1$); conversely, when placed at redshifts higher than $z \sim 1.5$, they would become among the most intrinsically luminous afterglows yet observed (Kouveliotou *et al.* 2004).

It is interesting to investigate how off-axis models apply to XRFs. Off-axis models predict that the early X-ray light curves will differ significantly from those of on-axis events. Specifically the light curves should start substantially fainter and then rise as the core of the on-axis material slows down and comes into the observer's line of sight. An observer at $\theta_{\rm obs} > \theta_0$, where θ_0 is the initial jet opening angle, sees a rising light curve at early times, peaking when the jet Lorentz factor is $\sim 1/\theta_{\rm obs}$, and approaching that seen by an on-axis observer, at later times. Therefore under this model we would expect to find that at the time of our X-ray observations the XRF afterglow luminosities, if located at $z > 1$, should be smaller than those of classical, on-axis GRBs. For XRF 020427 early *BeppoSAX* observations imply that the afterglow decayed approximately monotonically from an early stage, and thus is incompat-

ible with a sharp edge seen off-axis (see e.g. Ramirez-Ruiz & Madau 2004); the lack of early X-ray data for XRF 011030 prevents us from drawing quantitative conclusions. Another possibility for XRF 020427 is that the jet does not have sharp edges but wings of lower energy and Lorentz factor that extend to large θ. Such a picture of the jet is consistent with the relativistic studies of the collapsar model by Zhang, Woosley, & MacFadyen (2003) and Ramirez-Ruiz, Celotti & Rees (2002). The early emission detected by *BeppoSAX* in XRF 020427 would be then produced by material (on the wings) moving in our direction.

For a dirty fireball or an inefficient shock model the degree of collimation can be similar to that of a GRB, and an XRF can still be viewed directly down the jet-axis. The evolution of the XRF light curve could be similar to that of a classical GRB. Unfortunately the sparse multiwavelength afterglow coverage makes any quantitative analysis in this case unreliable. For XRF 011030, however, the observed modulation during the first ~ 14 days in the 4.86 GHz and 8.46 GHz data[17], and the swings in the radio spectral index, bear the signature of diffractive scintillation. If this is indeed the case then the angular size of the source must be less than the diffractive angle θ_d. For typical parameters and an observing frequency of 8.46 GHz, $\theta_d = 3$ microarcseconds. For a relativistic expanding fireball, the linear size of the source is $R = f\gamma^2 ct$ and the apparent size is R/γ (here γ is the Lorentz factor for the expanding shell, and the factor f depends on the dynamical details of the expanding fireball model (see e.g. Katz & Piran 1998)). Thus, the apparent size of the source is $f\gamma ct \leq 2 \times 10^{17}(f/4)(\gamma/2)(t/2\ \mathrm{weeks})$ cm. Taking the above-mentioned size of 3 microarcseconds for the fireball at about t =2 weeks post-burst, we can obtain a constraint on the distance to the source. Using a value of 72 km s^{-1} Mpc^{-1} for the Hubble constant, we find $z \gtrsim 0.25$.

GRB host galaxies show a broad range of absolute magnitudes and physical extents (e.g. Hogg & Fruchter 1999; Bloom, Kulkarni & Djorgovski 2002). For both XRF 011030 and 020427 the angular size and absolute magnitude lie within the range seen for GRB host galaxies across a broad range of redshifts ($0.1 < z < 2.5$). Thus we cannot use morphological or luminosity information to constrain the distances to these galaxies.

We post below several explanations by which the lack of a supernova component can be accounted for. The first option is that XRF 011030 and 020427 are accompanied by bright supernovae but lie at $z > 1.2$-1.5. At this redshift XRF 020427 would clearly violate the observed E_p-E_{iso} relationship reported by Amati *et al.* (2002), Lloyd-Ronning & Ramirez-Ruiz (2002) and subsequently Lamb *et al.* (2004) using data from *BeppoSAX*, *BATSE* and *HETE-II*, respectively. This relationship finds that in GRBs, $E_p \propto E_{iso}^{1/2}$. Under this scheme the isotropic energy of XRFs must be lower than that seen for GRBs, which would in turn result in a shorter distance distribution. To date it has been difficult to extend this relation into the XRF regime (especially at very low $E_p < 10$ keV) since only one XRF has a firmly established redshift (XRF 020903 at $z = 0.25$; Soderberg *et al.* 2003). However the existence of GRB/XRF 030429 at $z = 2.66$ (Jakobsson *et al.* 2004; Sakamoto *et al.* 2004) implies that some outliers do exist, although the $E_p = 35$ keV for this burst is not sufficiently low to be greatly constraining. Likewse the E_p limit on XRF 011030 of $E_p < 40$ keV does not provide a strong indicator of redshift. However for XRF 020427 the $E_p < 5$ keV does impose stronger limits. Amati *et al.* (2004) derive a best fit redshift range of $0.1 < z < 0.2$ for XRF 020427 and they notice that at the maximum allowed redshift ($z < 2.3$ based on the optical spectra of van Dokkum & Bloom 2003) XRF 020427 would not fit the E_p-E_{iso} relation since this would require $E_p > 100$ keV. We also find that if at $z > 0.5$, XRF 020427 lies outside the 90 % bounds of the Amati relation, assuming the latter is described by $E_p = 89(E_{iso}/10^{52})^{0.5}$ with a lognormal scatter of 0.3 (Butler *et al.* 2004). Notably GRB 980425, also violates this relationship, with a very low E_{iso} and high E_p. In contrast, should XRF 020427 be at higher-z, it would be the most extreme of the outliers with low E_p and high E_{iso}.

Another straightforward explanation would be that these XRFs were not accompanied by a luminous supernova. While this is possible, it is puzzling given the clear observational evidence for supernovae now seen in many low redshift, long duration GRBs, the possible association of an XRF with a supernova (XRF 030723; Fynbo *et al.* 2004) and the spectroscopic supernova signatures seen in GRB/XRF 031203.

Further possibilities which can explain *both* a low redshift and the absence of a supernova are, (i) that the afterglows were heavily dust extinguished, (ii) that the associated supernovae were very faint, or (iii) that the supernova and XRF were not temporally coincident in each of these cases. We now consider each of these options in turn.

In the high extinction scenario both afterglow and supernova would not be seen due to the strong absorption of optical light. The colors of their host galaxies, however, imply that they contain little dust. For XRF 020427, this is confirmed by deep K-band imaging that rules out very red colors; the limit is formally $R - K < 2.5$ (Bloom *et al.* 2003). The caveat here is that these observations do not probe the line of sight directly to the source of the burst, which could potentially be heavily extinguished. To investigate this possibility we have plotted in the bottom panel in Figures 3 & 4 the extinction necessary in the host galaxy of each XRF to hide a SN as strong as SN 1998bw and SN 2002ap. Here we have assumed an SMC like extinction law (Pei 1993), found to be the best fit to many GRB afterglows (e.g. Jakobsson *et al.* 2004; Holland *et al.* 2003). Similarly, the majority of GRBs do not show excessive extinction in their light curves and only GRB 030115 ($A_V \sim 1.5$) Levan *et al.* , in prep; Lamb *et al.* 2003) has a significant dust column. Thus if these two XRFs do demonstrate heavy reddening, then they are very different from the optically bright GRBs.

One way of determining the possible extinction along the line of sight is to measure the hydrogen column density (N_H) from the X-ray data. Each XRF has a relatively

[17] http://www.aoc.nrao.edu/∼dfrail/011030.dat

low number of counts (see Table 2) and therefore the limits which we can place are unfortunately poorly constrained. However in each case we find a value marginally in excess (but consistent with) the Galactic value. The 95 % upper limits on the value of N_H (Galactic + host galaxy) are $\sim 3.5 \times 10^{21}$ cm^{-2} and $\sim 4 \times 10^{21}$ cm^{-2} for XRF 011030 and XRF 020427, respectively. Accounting for the Galactic column and using Bohlin *et al.* (1978) to convert from N_H to A_V, this implies an upper limit on the host galaxy extinction of $A_V < 1.7$ and $A_V < 2.5$ for XRF 011030 and XRF 020427, respectively. These poorly constrained limits are also consistent with zero host galaxy extinction; we note, however, that the conversion between N_H and A_V is sensitive to the assumed dust to gas ratio and therefore somewhat uncertain.

Since the extinction required to remove a supernova signature at low redshift ($z < 0.5$) is very large and apparently incompatible with the measured dust columns it is logical to consider if a fainter supernova could explain these observations. Richardson *et al.* (2002) conducted a survey of the absolute magnitude distributions of all types of supernovae; they found that the faintest SN Ic peaked at approximately $M_V = -16$. Assuming a similar light curve evolution to SN 1998bw, such a SN would have been visible at $z \sim 1$ with no host galaxy extinction. As the supernova peak light scales linearly with its Ni yield, we would expect very little Ni production from a very faint supernova. The faintest local core collapse supernovae are of type II-P (again see Richardson *et al.* 2002), which approach $M_V \sim -14$; such supernovae would only be seen at low redshifts ($z < 0.5$). It is, however, by no means clear that such supernovae are capable of producing GRBs.

A final option is that the supernova and XRF are not temporally coincident. In the collapsar model (Woosley 1993) the GRB occurs within seconds of the supernova explosion, while other models have suggested that a longer delay could occur between the two events. For example in the supranova model (Vietri and Stella 1998) the GRB can be produced months to years after the SN. Long delays are however not favored by observations of low redshift GRBs which support simultaneous explosions (Galama *et al.* 1998; Hjorth *et al.* 2003; Stanek *et al.* 2003). At moderate redshifts, the supranova model may be a viable explanation for the lack of supernovae associated with XRF 011030 and 020427, as a supernova occuring a few weeks before the XRFs would not have been detected; at very low redshifts ($z < 0.2$) the delay would have to be over 6 months.

5. CONCLUSIONS

We have presented deep, multi-epoch *HST* observations of the fields of two XRFs. These observations, reaching depths of $V \sim 28.5$ would be sensitive enough to detect underlying supernovae such as SN 1998bw or SN 2002ap out to $z > 1$ even with moderate host galaxy extinction. At very low redshifts the extinction required to remove the supernova flux is very large, and incompatible with the measured column density in the case of XRF 020427. At higher redshifts XRF 020427 does not fit the E_p - E_{iso} relationship. This situation can be reconciled if the XRFs are situated locally behind large dust absorbing columns, if the supernovae are very faint, or if the SN and XRF are not temporally coincident. A final option is that GRBs and some XRFs do not represent the same physical process, and that they may be due to similar but physically distinct phenomena, where a supernova is not required for the latter.

The recent XRF 040701 may allow greater insights into the XRF-SN association, or the lack thereof. Optical observations failed to locate either a supernova or an optical afterglow (Berger *et al.* 2004; Pian *et al.* 2004), while *Chandra* observations did find a candidate X-ray afterglow (Fox *et al.* 2004) and a coincident galaxy system at low redshift $z = 0.22$. Deep *HST* observations of this object may significantly aid our understanding of the XRF phenomenon.

ACKNOWLEDGMENTS

Support for Proposal GO 9074 was provided by NASA through a grant from the Space Telescope Science Institute, which is operated by the Association of Universities for Research in Astronomy, Incorporated, under NASA contract NAS5-26555. This work is also based partly on observations made with the Chandra X-ray Observatory, and at the Wisconcin, Indiana, Yale, and National Optical Astronomy Observatories (WIYN), and the Danish 1.5m. telescope at La Silla, Chile under ESO program 69.D-0701. This work was conducted in part via collaboration within the the Research and Training Network "Gamma-Ray Bursts: An Enigma and a Tool", funded by the European Union under contract number HPRN-CT-2002-00294. A.J.L. acknowledges receipt of a PPARC studentship and support from the Space Telescope Science Institute Summer Student Program. S.K.P. acknowledges support from HST Grant Number GO 9074 and SAO grant number GO1-2055X. This work was also supported by the Danish Natural Science Research Council (SNF). We thank the referee for a prompt and constructive report.

REFERENCES

Amati, L., et al. 2002, A&A, 390, 81
Amati, L., et al. 2004, ArXiv Astrophysics e-prints, astro-ph/0407166
Atteia, J.-L. 2003, A&A, 407, L1
Barraud, C. et al. 2003, A&A, 400, 1021
Berger, E. et al. 2004, GRB Circular Network, 2631
Bersier, D., et al. 2004, GRB Circular Network, 2544
Bertin, G., Arnouts, S., 1996, A&AS, 117, 393B
Bloom, J. S., Kulkarni, S. R., & Djorgovski, S. G. 2002, AJ, 123, 1111
Bloom, J. S., Fox, D., van Dokkum, P. G., Kulkarni, S. R., Berger, E., Djorgovski, S. G., & Frail, D. A. 2003, ApJ, 599, 957
Bohlin, R. C., Savage, B. D., & Drake, J. F. 1978, ApJ, 224, 132
Butler, N. R., et al. 2004, ArXiv Astrophysics e-prints, astro-ph/0408453
Cash, W., Charles, P., Bowyer, S., Walter, F., Ayres, T. R., & Linsky, J. L. 1979, ApJ, 231, L137
Castro-Tirado, A., Gorosabel, J., Sanchez-Fernandez, C., Lund, N., Brandt, S., & Castro Ceron, J. M. 2002, GRB Circular Network, 1439

Cobb, B. E., Bailyn, C. D., van Dokkum, P. G., Buxton, M. M., & Bloom, J. S. 2004, ApJ, 608, L93
Christensen, L., Hjorth, J., Gorosabel, J., 2004, A&A, 425, 913
Dado, S., Dar, A. & De Rujula, A. 2004, A&A, 422, 381
Dermer, C. D., Chiang, J., & Bottcher, M. 1999, ApJ, 513, 656
Dickey, J. M. & Lockman, F. J. 1990, ARA&A, 28, 215
Foley, R. J., et al. 2003, PASP, 115, 1220
Fox, D. W. 2002a, GRB Circular Network, 1392
Fox, D. W. 2002b, GRB Circular Network, 1387
Fox, D. W., et al. 2003, ApJ, 586, L5
Fox, D.B., 2004, GRB Circular Network, 2630
Fruchter, A. S. & Hook, R. N. 2002, PASP, 114, 144
Fruchter, A., Patel, S., Kouveliotou, C., Rhoads, J., Holland, S., Burud, I., & Wijers, R. 2002a, GRB Circular Network, 1268
Fruchter, A., Rhoads, J., Burud, I., Levan, A., Patel, S., Kouveliotou, C., Gorosabel, J., & Hjorth, J. 2002b, GRB Circular Network, 1440
Fynbo, J. P U., et al. 2001, A&A, 369, 373
Fynbo, J. P. U., et al. 2004, ApJ, 609, 962
Galama, T. J., et al. 1998, Nature, 395, 670
Gal-Yam, A., et al. 2004, ApJ, 609, L59
Gandolfi, G. 2001, GRB Circular Network, 1119
Garnavich, P.M., et al., 2003, ApJ, 582, 924
Greiner, J. et al. 2003, ApJ, 599, 1223
Groot, P. J., *et al.* 1998, ApJ, 493, L27
Harrison, F. A., Yost, S., Fox, D., Heise, J., Kulkarni, S. R., Price, P. A., & Berger, E. 2001, GRB Circular Network, 1143
Heise, J., in't Zand, J., Kippen, R. M., & Woods, P. M. 2001a, Gamma-ray Bursts in the Afterglow Era, 16
Heise, J., in't Zand, J. J. M., Kulkarni, S. R., & Costa, E. 2001b, GRB Circular Network, 1138, 1
Hjorth, J., et al. 2003, Nature, 423, 847
Hogg, D. W. & Fruchter, A. S. 1999, ApJ, 520, 54
Holland, S. T., et al. 2003, AJ, 125, 2291
Huang, Y. F., Dai, Z. G., & Lu, T. 2002, MNRAS, 332, 735
in't Zand, J., Reali, F., Granata, S., Lowes, P., & Piro, L. 2002, GRB Circular Network, 1383
Jakobsson, P., et al. 2004, A&A, in press, astro-ph/0407439
Jakobsson, P., et al. 2004, ApJL, submitted
Katz, J. I., Piran, T. 1998, ApJ, 501, 425
Kouveliotou, C., Meegan, C. A., Fishman, G. J., Bhat, N. P., Briggs, M. S., Koshut, T. M., Paciesas, W. S., & Pendleton, G. N. 1993, ApJ, 413, L101
Kouveliotou, C., et al. 2004, ApJ, 608, 872
Lamb, D. Q., et al. 2004, New Astronomy Review, 48, 423
Lamb, D. Q., Donaghy, T. Q., & Graziani, C. 2003, ArXiv Astrophysics e-prints, astro-ph/0312634
Le Floc'h, E., et al. 2003, A&A, 400, 499
Levan, A. et. al. 2004, ApJ, submitted, astro-ph/0403450
Levan, A. et al. 2004, ApJ, in prep.
Lloyd-Ronning, N., & Ramirez-Ruiz, E. 2002, ApJ, 576, 101
Malesani, D., et al. 2004, ApJ, 609, L5
Mészáros, P. 2002, ARA&A, 40, 137
Mészáros, P., Ramirez-Ruiz, E., Rees, M. J., Zhang, B. 2002, ApJ, 578, 812
Millard, J., et al. 1999, ApJ, 527, 746
Patat, F., et al. 2001, ApJ, 555, 900
Pei., Y.C. 1992, ApJ, 395, 130
Pian, E. et al. 2004, GRB Circular Network, 2638
Preece, R. D., Briggs, M. S., Mallozzi, R. S., Pendleton, G. N., Paciesas, W. S., & Band, D. L. 2000, ApJS, 126, 19
Price, P. et al. 2003, ApJ, 584, 931
Ramirez-Ruiz, E., Lloyd-Ronning, N. M. 2002, New Astron., 7, 197
Ramirez-Ruiz, E., Celotti, A., & Rees, M. J. 2002, MNRAS, 337, 1349
Ramirez-Ruiz, E., & Madau, P. 2004, ApJ, 608, L89
Rhoads, J. E. 2003, ApJ, 591, 1097
Rhoads, J. E., Burud, I., Fruchter, A., Kouveliotou, C., & Wood-Vasey, W. M. 2001, GRB Circular Network, 1140
Richardson, D. Branch, D., Casebeer, D., Millard, J., Thomas, R.C., Baron, E., 2002 ApJ123, 745
Rol, E. et al. 2004, ApJ, in prep.
Sakamoto, T., et al. 2004, ArXiv Astrophysics e-prints, astro-ph/0409128
Sazonov, S., Lutovinov, A., & Sunyaev, R. 2004, Nature, 430, 646
Schlegel, D. J., Finkbeiner, D. P., & Davis, M. 1998, ApJ, 500, 525
Soderberg, A. M., et al. 2004, ApJ, 606, 994
Stanek, K. Z., et al. 2003, ApJ, 591, L17
Taylor, G. B., Frail, D. A., & Kulkarni, S. R. 2001, GRB Circular Network, 1136
Thomsen, B., et al. 2004, A&A, 419, L21
Trentham, N., Ramirez-Ruiz, E., & Blain, A. W., 2002, MNRAS, 334, 983
van Dokkum, P. G. & Bloom, J. S. 2003, GRB Circular Network, 2380
Vaughan, S., et al. 2004, ApJ, 603, L5
Vietri, M. & Stella, L. 1998, ApJ, 507, L45
Watson, D., et al. 2004, ApJ, 605, L101
Woosley, S. E. 1993, ApJ, 405, 273
Wieringa, M. H., Berger, E., Fox, D. W., & Frail, D. A. 2002, GRB Circular Network, 1390
Yamazaki, R., Ioka, K., & Nakamura, T. 2002, ApJ, 571, L31
Zeh, A., Klose, S., & Hartmann, D. H. 2004, ApJ, 609, 952
Zhang, B. & Mészáros, P. 2002, ApJ, 581, 1236
Zhang, W., Woosley, S. E., & MacFadyen, A. I. 2003, ApJ, 586, 356

TABLE 1
Chandra OBSERVATIONS OF XRF 011030, XRF 020427

Date	Δt^b	t_{exp} (ks)	Counts^c	Γ	N_H (10^{21} cm^{-2})	F_x^c
XRF 011030						
2001 Nov 09.728	10.46	46.6	374	1.31(8)	1.02	1.06×10^{-13}
2001 Nov 29.464	30.19	19.9	16	1.3(4)	1.02	1.07×10^{-14}
XRF 020427						
2002 May 06.225	9.08	13.7	56	1.3(2)	0.29	5.1×10^{-14}
2002 May 14.154	17.00	14.6	24	2.1(3)	0.29	1.2×10^{-14}

NOTE.—^{a} values in parenthesis correspond to 68% uncertainty, ^{b} days since burst, ^{c} measured counts and unabsorbed flux (erg s^{-1} cm^{-2}) between $0.3 - 10$ keV, ^{d} Galactic value (Dickey & Lockman ,1990) , indicates that the spectral index is determined by a joint fit to both data sets.

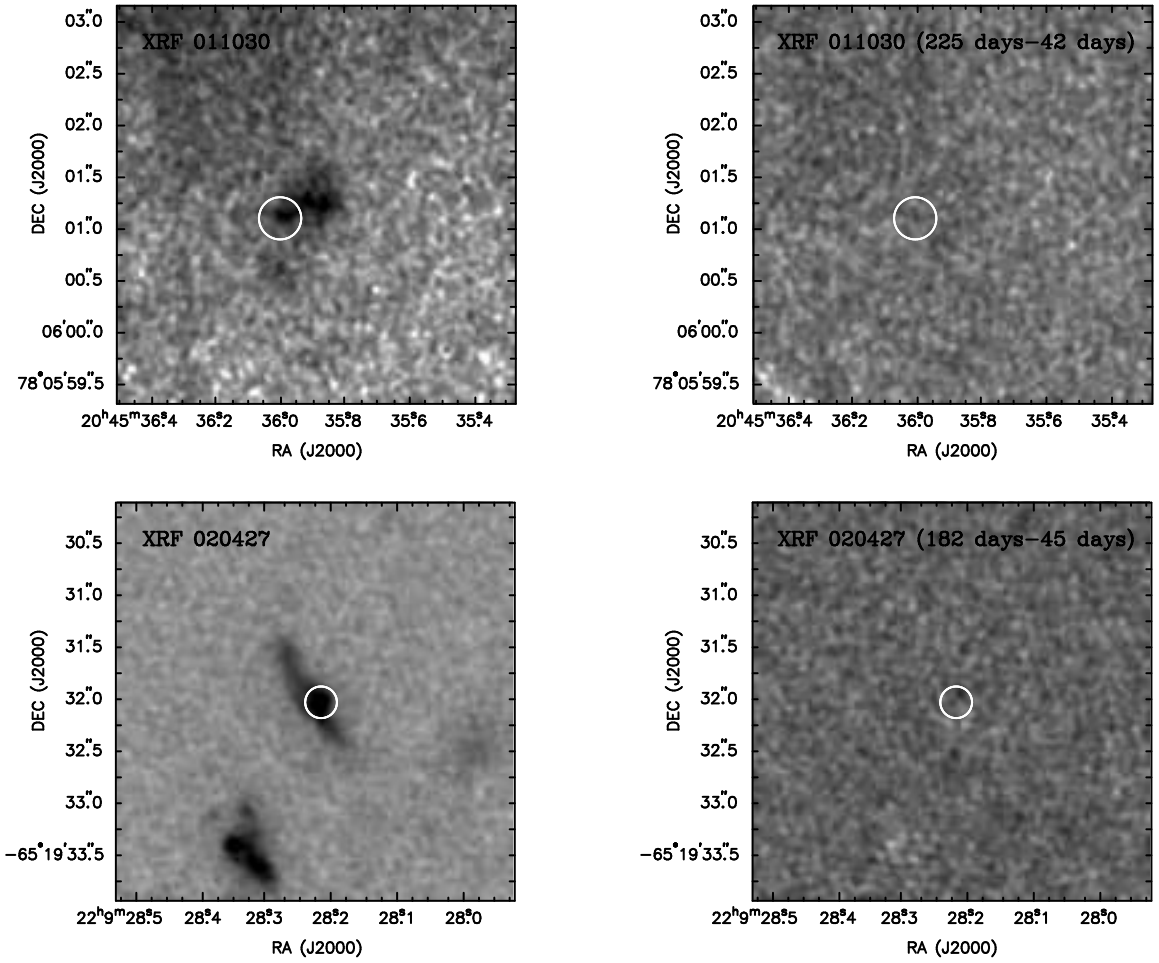

FIG. 1.— The host galaxies of XRFs 011030 and 020427 (left column) and the results of difference imaging on each of their fields (right column). For each XRF the images were obtained with STIS. The two subtracted images are taken approximately six months apart and show no evidence for any excess emission at either epoch, placing limits of $V \sim 28.5$ for the combination of afterglow and supernovae approximately 40 days after each burst. In each image North is up, and East to the left.

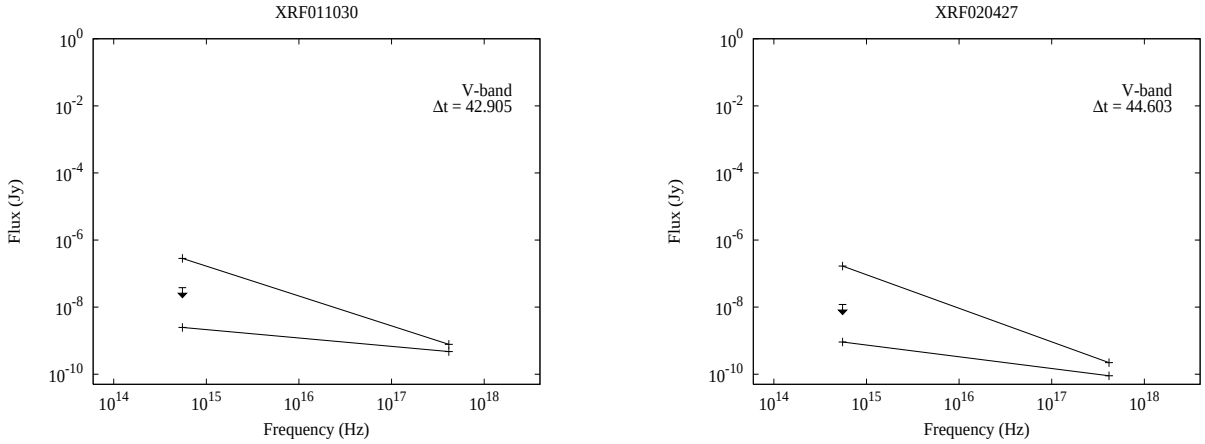

FIG. 2.— The extrapolation of the X-ray afterglows of XRF 011030 (left) and XRF 020427 (right) into the optical waveband (STIS). The optical limits shown are derived from extrapolating the X-ray observations both temporally and spectrally to the optical observations. This was done using the powerlaw indices from the X-ray observations, and allowing for a possible cooling or jet break between the epoch of the X-ray and optical observations, such that the final optical limits derived are the extremes of all possible allowed scenario's (see Rol *et al.*2004).

TABLE 2
OPTICAL OBSERVATIONS OF XRF 011030, XRF 020427 AND THEIR HOST GALAXIES

Date	$\Delta t = t - t_0$ (days)	Inst./Filter	Exp. Time (s)	mag.
XRF 011030				
2001 Nov 1.221	0.952	WIYN/R	3000	> 22.5
2001 Nov 3.132	2.862	WIYN/R	3000	> 22.2
2001 Dec 12.175	42.905	STIS/50CCD	8640	25.31 ± 0.10
2002 June 12.602	225.380	STIS/50CCD	7505	25.30 ± 0.10
XRF 020427				
2002 May 11.607	14.447	Danish 1.54m/I	2700	> 22.0
2002 June 10.762	44.603	STIS/50CCD	8640	24.44 ± 0.05
2002 June 14.734	48.575	STIS/50CCD	4781	24.45 ± 0.05
2002 Oct 26.011	181.852	STIS/50CCD	8392	24.44 ± 0.05

NOTE.—Photometry measure is of the host galaxy. All photometry is corrected for galactic extinction. For R and I band observations the corrections are based on the values of Schlegel, Finkbeiner & Davis (1998). For the broad band 50CCD images we estimate the extinction based on the change in count rate observed for a typical GRB host galaxy spectral slope of $\nu^{-0.8}$ when folded through the 50CCD passband. The corresponds to $A_{50CCD} = 1.17$ and 0.06 for XRF 011030 and 020427 respectively.

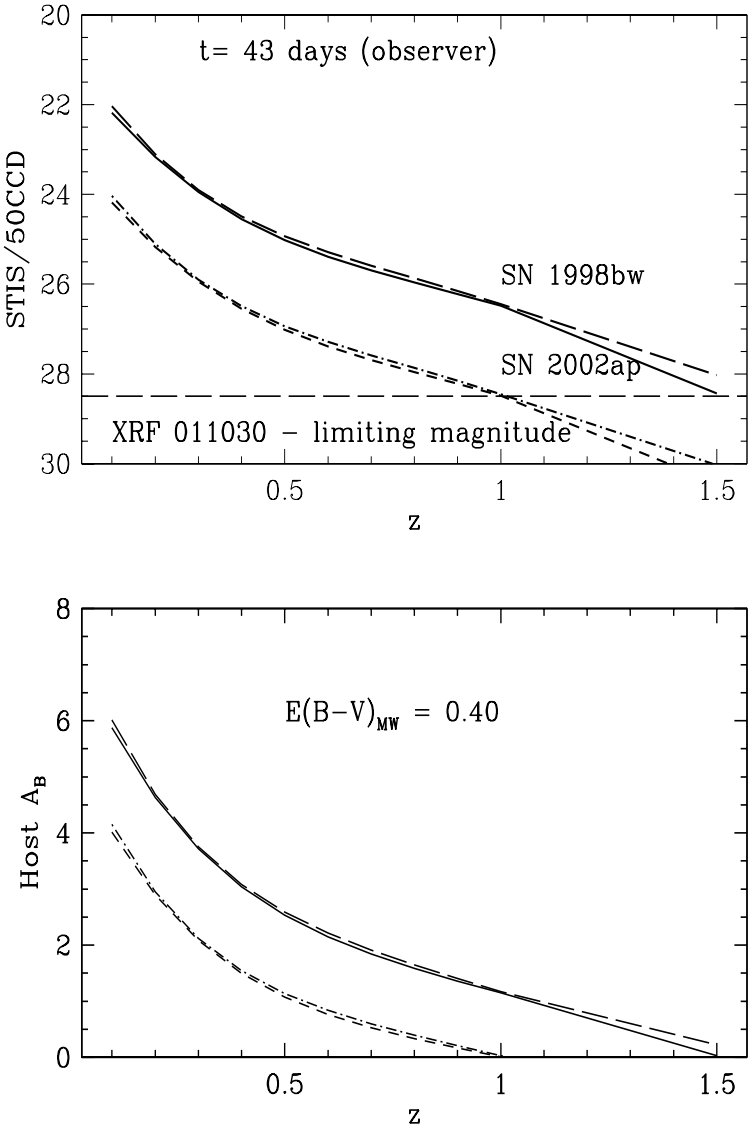

FIG. 3.— *upper panel*: Evolution of the magnitude of SN 1998bw and SN 2002ap at various redshifts in the XRF 011030 field and at a fixed observer time. Two lines are shown for each supernova, the lower line (solid for SN 1998bw, dashed for SN 2002ap) show the extrapolations assuming zero flux for $\lambda < 3000$Å, while the upper line shows the magnitudes assuming that the UV-flux had a spectral shape as determined from SN 2002ap. The horizontal line corresponds to the limiting XRF magnitude calculated in this paper. *bottom panel*: The required rest frame B-band extinction within each XRF host galaxy such that either a 1998bw or a 2002ap like SN could be hidden. The two lines again represent different methods of treating the UV component of the supernova flux.

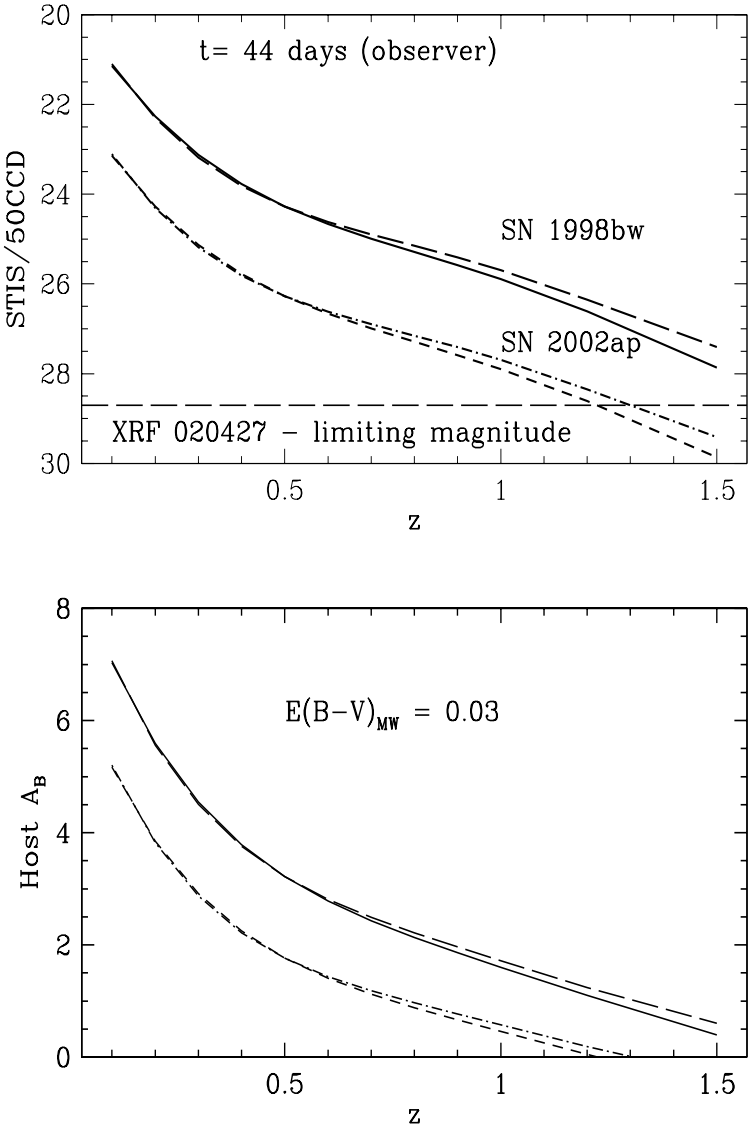

FIG. 4.— As for Figure 3, but for the XRF 020427 field. Note the limits shown in each figure (dashed line in the upper panel) are the raw observed limits not corrected for Galactic extinction, since the extinction is considered when the spectra are folded through the instrument response. (i.e. the expected magnitude plotted in the upper panel is that expected for the Galactic extinction relevant for each XRF).